IEEE Access
Multidisciplinary | Rapid Review | Open Access Journal

Date of publication xxxx 00, 0000, date of current version xxxx 00, 0000.

Digital Object Identifier 10.1109/ACCESS.2017.Doi Number

Dual Output and High Voltage Gain DC-DC Converter for PV and Fuel Cell Generators Connected to DC Bipolar Microgrids

V. Fernão Pires[1,3], Senior, IEEE, Armando Cordeiro [2,3], Daniel Foito[1,4] and J. Fernando Silva[3,5], Senior, IEEE

[1] SustainRD, ESTSetúbal, Polytechnic Institute of Setúbal, Setúbal 2914–508, Portugal
[2]ISEL, Polytechnic Institute of Lisbon, Lisbon 1959–007, Portugal
[3]INESC-ID, Lisbon 1049-001, Portugal
[4]CTS-UNINOVA, New University of Lisbon, Caparica 2829-516, Portugal
[5]IST, University of Lisbon, Portugal

Corresponding author: V. Fernão Pires (e-mail: vitor.pires@estsetubal.ips.pt).

This work was supported by national funds through FCT Fundação para a Ciência e a Tecnologia with reference UIDB/50021/2020 and UIDB/00066/2020.

ABSTRACT This paper introduces a new topology for a *DC-DC* converter with bipolar output and high voltage gain. The topology was designed with the aim to use only one active power switch. Besides the bipolar multiport output and high voltage gain this converter has another important feature, namely, it has a continuous input current. Due to the self-balancing bipolar outputs, the proposed topology is suitable for bipolar *DC* microgrids. Indeed, the topology balancing capability can achieve the two symmetrical voltage poles of bipolar *DC* microgrids. Furthermore, it is possible to create a midpoint in the output of the converter that can be directly connected to the ground of the *DC* power supply, avoiding common-mode leakage currents in critical applications such as transformerless grid-connect *PV* systems. The operating principle of the proposed topology will be supported by mathematical analysis. To validate and verify the characteristics of the presented topology, several experimental results are shown.

INDEX TERMS Photovoltaic (*PV*) systems, Fuel Cell, *DC-DC* converter, Bipolar *DC* microgrid, Single-switch.

I. INTRODUCTION

Energy conversion systems are extremely important for modern societies and are present in different forms in most domestic, commercial and industrial applications [1]. With the increasing challenges of CO_2 reduction and proliferation of solutions using clean and renewable resources (e.g. electrification of transport or photovoltaic systems), the importance and interest around power electronic converters has grown strongly over the last decades [2]. Numerous power converters have been proposed over the years to overcome different integration problems and, at the same time, improve different economic and operational aspects of such systems. Among all power converters, the *DC-DC* converter is currently one of the most important electronic circuit in the overall decarbonization process allowing to mitigate problems with integration of renewable energy sources (*RES*) [3], smart grids [4], integration and optimization of storage devices [5], electric vehicles [6], battery chargers [7] and many others. Some of the most desired characteristics of *DC-DC* converters are high-efficiency, cost effectiveness and the voltage regulation capability in order to allow a wide range of applicability. For certain applications, the step-up voltage of the classic *DC-DC* converters can be a simple and acceptable solution [8] [9]. However, for applications where a high step-up ratio is required other *DC-DC* converters have been reported in literature. In general *DC-DC* converters are classified into two main categories: isolated and non-isolated topologies [10]. Some isolated solutions are based on a single-switch and a high frequency transformer using either hard or soft-switching resonant or quasi-resonant circuits [10] [11]. Other isolated solutions using multiple switches, high frequency transformers, quasi-Z source topologies and soft

This article has been accepted for publication in a future issue of this journal, but has not been fully edited. Content may change prior to final publication. Citation information: DOI 10.1109/ACCESS.2021.3122877, IEEE Access

switching techniques can be found in [12]-[14]. Other topologies are based on the boost full-bridge [15] [16], isolated push-pull boost [17] and isolated inductor-feed boost converter [18]. Using isolated converters, it is possible to achieve relatively high voltage regulation ratios and, in some cases, high efficiency by properly designing the transformer's turn ratio and the soft-switching circuits. The costs associated with the high number of switching devices and transformers, in addition to more complicated control schemes and more isolated sensors are some of the main drawbacks of these isolated topologies. Some existing isolated voltage-type converters also present pulsed input current, which negatively impacts the life of *PV* arrays. Several non-isolated topologies have also been proposed to extend the output to input voltage transfer ratio (voltage gain) of existing boost converters. Some advantages and applications of non-isolated topologies can be found in [9] [19]. Some topologies are based on the integration of different *DC-DC* converters and use a single switch [20]-[22]. Other high step-up voltage converters are based on coupled inductors [23] [24]. These solutions represent a simple, effective, and promising alternative to achieve a wide range of voltage conversion. Other high step-up voltage converters are based on switched inductors and switched capacitors cells [25]-[28]. Some solutions to achieve high step-up voltage ratios are based on voltage-multiplier or voltage-lift techniques [29]-[31]. Quadratic boost converters and quasi-Z source topologies also provide another effective method to obtain high-step-up voltage gains [32]-[36]. These converters have usually less volume, simpler circuits and are more suitable for extreme voltage applications. Despite several advantages of non-isolated boost converters, some require multiple switching devices to achieve high-step-up voltage gains, which increase the cost and complexity. Some converters require only a single switching device but present limited voltage gain. In practical terms, due to large parasitic capacitors at the ground of the *PV* panels, the leakage current in the non-isolated *PV* grid-connected system is an important issue and a key problem. A review of non-isolated high step-up *DC-DC* converters for *PV* applications regarding these issues can be found in [37].

Very important applications of *DC-DC* converters can be found in the context of the *DC* microgrids. Main architectures of *DC* microgrids include the unipolar and bipolar wiring configurations. The bipolar architecture microgrid has two poles presenting symmetrical voltages regarding a ground pole and is becoming attractive due to several advantages such as, higher resilience, increased efficiency and power supply with higher quality [38]. However, bipolar microgrids can suffer from an important disadvantage, namely the bipolar voltage unbalance. Unbalances are due to the connection of loads with different power or characteristics to the two poles whose voltage variation departs from the voltage symmetry. To eliminate or attenuate this disadvantage solutions like the use of voltage balancers were proposed [39] [40]. However, this approach requires an extra power converter, increasing the cost and losses of the system. Better solutions require that the *DC-DC* generators balance the bipolar *DC* microgrid voltages. To achieve this, the use of converters with dual outputs, a common connection and symmetrical voltage outputs are needed [41]-[46]. However, these solutions normally require extra switches and/or have limited voltage gain.

In this paper a new *DC-DC* converter indicated to be used in bipolar *DC* microgrids is proposed hereafter. To be able to balance bipolar microgrids voltages the proposed topology outputs dual symmetrical voltages. Besides, the converter has also been designed to offer a very high voltage gain and continuous input current using only a single active switch. Therefore, the proposed converter is extremely suited for RES such as PV and fuel cell generators. Also, the proposed design allows a relatively reduced voltage stress across all power semiconductors of the *DC-DC* converter. The topology is also suitable for use in transformerless grid-connect solar *PV* and fuel cell generators. The design and analysis of the converter will be addressed in detail in the next sections. Some experimental results from a laboratory prototype are presented to confirm the theoretical validity of proposed converter.

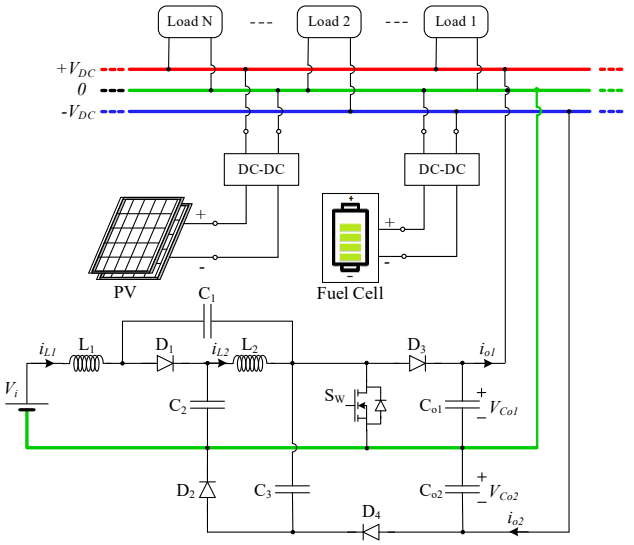

FIGURE 1. Power circuit configuration of the proposed *DC-DC* converter connected to bipolar *DC* microgrid.

II. DESCRIPTION OF THE PROPOSED DC-DC CONVERTER

To mitigate voltage unbalances in bipolar *DC* microgrids, *DC-DC* converters of *RES* applications, like *PV* and fuel cell generators, must be able to inject the power into the two poles of the microgrid as a way to balance the bipolar voltages. Thus, the proposed converter has dual outputs V_{Co1} and V_{Co2} illustrated in Fig. 1. Besides the important advantage of self-balancing the bipolar *DC* microgrid, the

This article has been accepted for publication in a future issue of this journal, but has not been fully edited. Content may change prior to final publication. Citation information: DOI 10.1109/ACCESS.2021.3122877, IEEE Access

proposed converter has high voltage gain and continuous input current. The proposed converter power circuit needs only a single active switch (S_w), two inductors (L_1 and L_2), three capacitors (C_1, C_2 and C_3) and four diodes (D_1 to D_4). From circuit analysis it is verified that the active switch does not withstand all the load voltage, given by the sum of the voltages across the output capacitors C_{o1} and C_{o2}.

The proposed circuit is also suited for applications like grid connected solar *PV* and fuel cell generators. One of the problems associated to the use of *DC-DC* converters in *PV* and fuel cell applications with transformerless inverter is the common mode leakage current. So, similar to previous case, the ground of the *PV* panel (or fuel cell) is directly connected to the neutral of the *AC* grid (green line of Fig. 2).

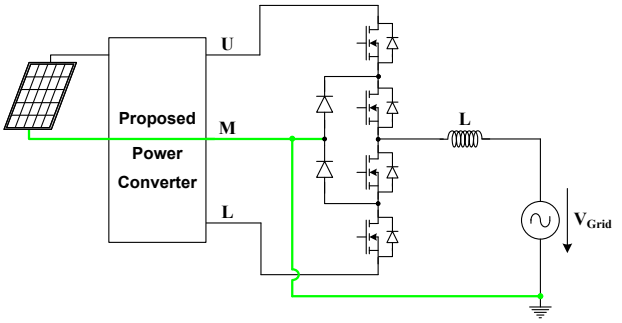

FIGURE 2. Connection of the proposed *DC-DC* converter to a half-bridge three level single phase inverter for transformerless *PV* applications.

III. ANALYSIS AND OPERATING PRINCIPLE OF THE PROPOSED DC-DC CONVERTER

As mentioned before, the circuit allows for continuous input current and high voltage gain. This can be verified through the analysis of the circuit in steady state behaviour and considering operation in the continuous conduction mode (*CCM*). In accordance with these assumptions, there are two possible operating modes, each one associated to one equivalent circuit (Fig. 4). The main waveforms of the voltages and currents in this circuit that are associated to the two operating modes are shown in Fig. 3.

From the analysis of the circuit the behaviour of the converter for each operating mode is described as follows:

- *Operating Mode I (time interval t_o-t_1)*: During this interval the turn *ON* voltage is applied in the gate of the transistor, resulting on the equivalent circuit of Fig. 4 a). Thus, inductors L_1 and L_2 have a positive voltage (input voltage source plus C_2 capacitor voltage and C_1 capacitor voltage) increasing their currents. The current in inductor L_1 will flow through capacitor C_1 (discharging it), transistor S_W and voltage source V_i. The current in the inductor L_2 will flow through transistor *SW* and capacitor *C2* (discharging it). The discharge of the capacitor C_3 depends of the output buses. Thus, if the voltage in capacitor C_{o1} is lower than capacitor C_{o2}, since the voltage of capacitor C_3 is approximately equal to the capacitor C_{o1} then there will be no discharge of capacitor C_3 over the capacitor C_{o2} since diode D_4 is reverse biased. Otherwise, capacitor C_3 will discharge over C_{o2} flowing the current through those capacitors and transistor S_W (see ② in Fig. 4 a)).

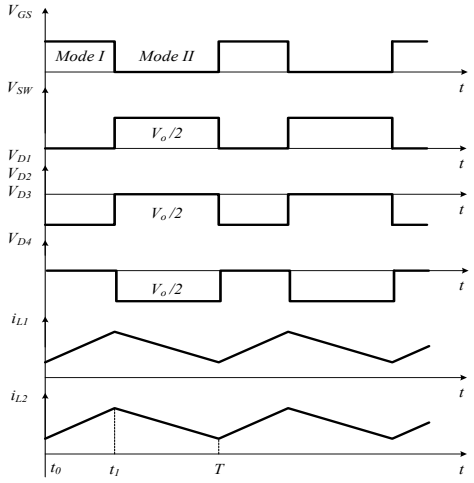

FIGURE 3. Main Waveforms associated to the operating modes of the proposed *DC-DC* converter.

From the analysis of this operating mode I, the following expressions are obtained by:

$$\begin{cases} v_{L_1} = L_1 \dfrac{di_{L_1}}{dt} = V_i + v_{C_1} \\ v_{L_2} = L_2 \dfrac{di_{L_2}}{dt} = v_{C_2} \\ v_{C_{o2}} = v_{C_3} \end{cases} \quad (1)$$

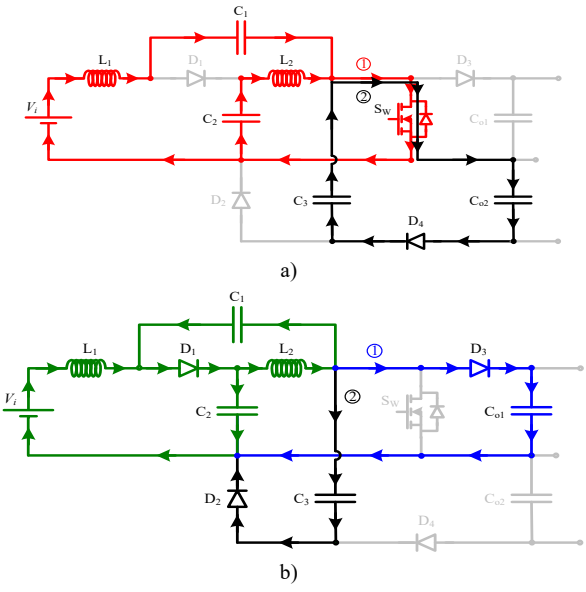

FIGURE 4. Equivalent circuits associated to each of the operating modes: a) time interval ($t_o < t < t_1$), b) time interval ($t_1 < t < T$).

This article has been accepted for publication in a future issue of this journal, but has not been fully edited. Content may change prior to final publication. Citation information: DOI 10.1109/ACCESS.2021.3122877, IEEE Access

- *Operating Mode II (time interval t_1-T)*: In this time interval the transistor S_W is turned *OFF*, originating the equivalent circuit presented in Fig. 4 b). The voltages across the inductors are now negative, forcing the currents in inductor L_1 and L_2 to decrease (discharge of the inductors). The current in the inductor L_1 will flow now through diode D_1, capacitor C_2 (charging it) and voltage source V_i. The current in the inductor L_2 will flow through capacitor C_1 (charging it) and diode D_1. The charge of the capacitor C_{o1} depends on the output buses. Thus, if the voltage in capacitor C_{o1} is lower than capacitor C_{o2} then (since the voltage of capacitor C_3 is approximately equal to the capacitor C_{o2}) there will be no charge of capacitor C_3 since diode D_2 is reverse biased. In this condition there will be a current flowing through this capacitor charging it (① in Fig. 4 b)). Otherwise, there will be a current flowing through capacitor C_3 charging it (② in Fig. 4 b)). In this operating mode the following expressions are obtained by:

$$\begin{cases} v_{L_1} = L_1 \dfrac{di_{L_1}}{dt} = V_i - v_{C_2}; v_{L_2} = L_2 \dfrac{di_{L_2}}{dt} = v_{C_1} \\ v_{C_{o1}} = v_{C_2} + v_{L_2} = v_{C_2} + L_2 \dfrac{di_{L_2}}{dt} \end{cases} \tag{2}$$

The voltage gain of this power converter topology can be determined from the analysis of the described two operating modes. Taking into consideration these modes and that the average value of voltages of the two inductors in steady-state are equal to zero, it is possible to obtain:

$$\begin{cases} \dfrac{1}{T}\displaystyle\int_0^T v_{L_1} dt = \frac{1}{T}\left[\int_0^{t_1} (V_i + v_{C_1})dt + \int_{t_1}^{T} (V_i - v_{C_2})dt\right] = 0 \\ \dfrac{1}{T}\displaystyle\int_0^T v_{L_2} dt = \frac{1}{T}\left[\int_0^{t_1} v_{C_2} dt - \int_{t_1}^{T} v_{C_1} dt\right] = 0 \end{cases} \tag{3}$$

Also considering that the capacitors C_1 and C_2 are sufficiently large, it can be assumed that the voltages at their terminals will change linearly, as well as, their average values, given by:

$$\begin{cases} V_{C_1} = \dfrac{1}{T}\displaystyle\int_0^T v_{C_1} dt = \frac{1}{t_1}\int_0^{t_1} v_{C_1} dt = \frac{1}{T - t_1}\int_{t_1}^{T} v_{C_1} dt \\ V_{C_2} = \dfrac{1}{T}\displaystyle\int_0^T v_{C_2} dt = \frac{1}{t_1}\int_0^{t_1} v_{C_2} dt \end{cases} \tag{4}$$

Using these last two equations in equations (3), it will be derived the equations that are described by:

$$\begin{cases} t_1(V_i + V_{C_1}) + (T - t_1)(V_i - V_{C_2}) = 0 \\ t_1 V_{C_2} - (T - t_1) V_{C_1} = 0 \end{cases} \tag{5}$$

From these equations and considering $\delta = (t_1/T)$ the duty cycle associated to the switch S_w, the average voltages of V_{C1} and V_{C2} are obtained by:

$$\begin{cases} V_{C_1} = \dfrac{t_1}{(T - t_1)^2 - t_1^2} V_i = \dfrac{\delta}{1 - 2\delta} V_i \\ V_{C_2} = \dfrac{T - t_1}{(T - t_1)^2 - t_1^2} V_i = \dfrac{1 - \delta}{1 - 2\delta} V_i \end{cases} \tag{6}$$

Using these equations with (1) and (2), the average value of the output capacitor voltages (or pole voltages) function of the input voltage will be determined by:

$$V_{C_{o1}} = V_{C_{o2}} = \frac{1}{1 - 2\delta} V_i \tag{7}$$

From the voltage gain given by this last equation it is foreseen that the proposed topology extends the voltage gain to the double of the conventional quasi-Z *DC-DC* converter, or obtains two outputs with the same gain.

IV. DESIGN OF THE POWER CONVERTER COMPONENTS

To determine the power semiconductors ratings, it will be considered again the converter operating in CCM with no losses. Thus, in steady state operation the next relationship is given:

$$P_i = P_o = V_i I_i = V_o I_o \tag{8}$$

where the current variables Ii and Io are the average value of the input voltage source and output load current.

Considering the relationship of the last expression and the gain voltage of the converter given by (7), the average value of the input current source is a function of the duty cycle and output load current, being given by equation (9). This expression also gives the average value of the inductor currents of the power converter.

$$I_i = I_{L_1} = I_{L_2} = \frac{2}{1 - 2\delta} I_o \tag{9}$$

For the design of the inductors and capacitors, it will be considered that they depend of the rated voltages and currents and that they ensure small ripple for the current in the inductors and voltage across the capacitors. Thus, considering the differential equation that represents the evolution of the current in the inductors (10) and the voltage across the inductor almost constant, the linear solution (11) is obtained. From this last equation considering equation (10) and $\Delta i_T = i_T(t) - i_T(t_o)$, the new relationship given by (12) is obtained.

This article has been accepted for publication in a future issue of this journal, but has not been fully edited. Content may change prior to final publication. Citation information: DOI 10.1109/ACCESS.2021.3122877, IEEE Access

$$\frac{di_L(t)}{dt} = \frac{v_L(t)}{L} \tag{10}$$

$$i_L(t) = \frac{v_L}{L} t_1 + i_L(t_o) \tag{11}$$

$$\frac{\Delta i_L}{t_1} = \frac{v_L}{L} \tag{12}$$

$$\begin{cases} L_1 = \dfrac{t_1(V_i + V_{C_1})}{\Delta I_{L_1}} = \dfrac{\delta(1-\delta)V_i}{(1-2\delta)f_s \Delta I_{L_1}} \\ L_2 = \dfrac{t_1 V_{C_2}}{\Delta I_{L_2}} = \dfrac{\delta(1-\delta)V_i}{(1-2\delta)f_s \Delta I_{L_2}} \end{cases} \tag{13}$$

To size the capacitors, a similar approach is used. Thus, considering the differential equation that mathematically represents the behavior of the capacitors voltage and the currents through the capacitors constant during the operation interval, the following relationship is obtained:

$$\frac{\Delta v_C}{\Delta t} = \frac{i_C}{C} \tag{14}$$

From the previous relationship, the capacitors depend on average currents of the capacitors and the time interval (t_1-T):

$$\begin{cases} C_{o1} = C_{o2} = \dfrac{t_1 I_o}{\Delta V_{C_{o1,o2}}} = \dfrac{\delta I_o}{f_s \Delta V_{C_{o1,o2}}} \\ C_1 = \dfrac{t_1 I_{C_1}}{\Delta V_{C_1}} = \dfrac{2\delta I_o}{(1-2\delta) f_s \Delta V_{C_1}} \\ C_2 = C_3 = \dfrac{t_2 I_{C_2}}{\Delta V_{C_2}} = \dfrac{(1-\delta) I_o}{f_s \Delta V_{C_2}} \end{cases} \tag{15}$$

The determination of the power semiconductors current stress can be done considering the average values of the currents in inductors and from the condition that the average values of the currents in each of the capacitors are zero in a switching cycle (T), giving:

$$\begin{cases} I_{S_w} = \left(\dfrac{4\delta}{1-2\delta} + \dfrac{1}{\delta}\right) I_o ; I_{D_1} = \left[\dfrac{4(1-\delta)}{1-2\delta} + \dfrac{1}{1-\delta}\right] I_o \\ I_{D_2} = I_{D_3} = \dfrac{1}{1-\delta} I_o ; I_{D_4} = \dfrac{1}{\delta} I_o \end{cases} \tag{16}$$

These equations show that the current in the switch is higher than the load current, as expected since the switch voltage stress is lower than the load voltage.

To determine the voltages stress across the semiconductors, it is considered that the voltage ripple across the capacitors can be neglected. The voltages in the power semiconductors are dependent on the capacitors voltages as written in (17). These expressions show that the voltage stresses of the power semiconductors are only half of the converter output voltage.

$$\begin{cases} V_{S_W} = V_{D_3} = V_{C_{o1}} = \dfrac{V_o}{2} ; V_{D_1} = V_{C_1} + V_{C_2} = \dfrac{V_o}{2} \\ V_{D_2} = V_{D_4} = V_{C_{o2}} = \dfrac{V_o}{2} ; V_{D_3} = V_{C_{o1}} = \dfrac{V_o}{2} \end{cases} \tag{17}$$

V. EFFECTS OF NON-IDEALITIES OF THE INDUCTORS

The non-idealities of the circuit components will affect the voltage gain of the power converter. The elements that have more impact on that are the inductors. To verify that impact, the circuit will be analyzed considering that the losses in those inductors can be represented by an equivalent resistance. In this way, associated to those inductors will be considered that the resistances of r_{L1} and r_{L2} are in serial connection with the inductors L_1 and L_2, respectively. For the analysis of the power circuit in non-ideal conditions with the previous assumptions, the load was considered as an equivalent resistance R_0. Thus, with all these considerations it is obtained the static voltage gain of the converter, expressed by:

$$\frac{V_{DC\_bus}}{V_{St}} = \frac{2}{\dfrac{r_{L1}}{R_o}\dfrac{(4-8\delta)}{(1-2\delta)^2} + \dfrac{r_{L2}}{R_o}\dfrac{(4-8\delta)}{(1-2\delta)^2} + (1-2\delta)} \tag{18}$$

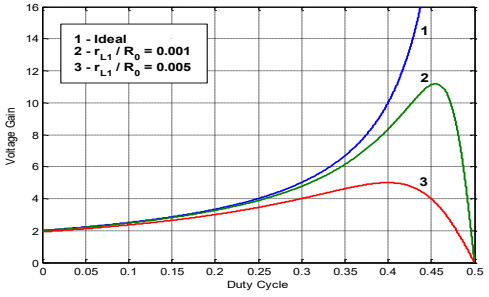

FIGURE 5. Static voltage gain ratio function of the duty-cycle in non-ideal conditions.

To verify the impact of the inductors and load resistances, it is shown in Fig. 5 the voltage gain of the converter as a function of the duty cycle for different values of $r_{L1} / R_0 = r_{L2} / R_0$. From Fig. 5 it is seen that the voltage gain is limited. This limitation is function of the resistors values. Considering for example $r_{L1} / R_0 = r_{L2} / R_0 = 0.001$, the maximum voltage gain will be around 11, while if it is considered $r_{L1} / R_0 = r_{L2} / R_0 = 0.005$, the maximum voltage gain is reduced to 5.

VI. SIMULATION AND EXPERIMENTAL TESTS

The proposed *DC-DC* converter based on a quasi-Z topology with extended voltage gain and dual output characteristic was subject to simulation and experimental tests. For the experimental tests it was developed a prototype with

This article has been accepted for publication in a future issue of this journal, but has not been fully edited. Content may change prior to final publication. Citation information: DOI 10.1109/ACCESS.2021.3122877, IEEE Access

demonstrating purposes regarding their operating principle and confirmation of their features. The simulation and experimental tests were made in accordance with Fig. 1, in which inductors L_1 and L_2 have 1,1 mH, and capacitors of 100 µF, 68 µF and 68 µF are used for C_1, C_2 and C_3 respectively. For the output capacitors C_{01} and C_{02} have a capacitance of 470 µF. The load connected to the power converter consists in a 540 Ω resistor. The power converter is supplied by a *DC* power source with 60 V and was operated with a switching frequency of 20 kHz. The duty cycle was adjusted to obtain an output voltage of 400 V.

A. SIMULATION TESTS

The obtained simulation results for a duty cycle of 0.35 are presented in Figs. 6 to 8. Fig. 6 presents the voltage waveforms of the input (V_i) and outputs (V_{Co1}, V_{Co2} and V_o) of the proposed power converter. In accordance with the defined duty cycle, it is expected a theoretical gain of 6.7. Analysing this figure is possible to verify that a similar gain is obtained. Besides that, it is possible to confirm that the voltages of the output capacitors (C_{o1} and C_{o2}) have practically the same average value equal to half of the total output voltage. The voltages across the power semiconductors can be seen in Fig. 7 where the waveforms that were obtained through this simulation test are presented. The analysis of these waveforms confirms that the voltage across semiconductors is lower than the output voltage. They are in accordance with the described in the theoretical analysis, being half of the total output voltage. The input current (also in the inductor L_1), inductor current L_2 and output current are presented in Fig. 8. From these waveforms obtained from the simulation test, it is possible to confirm the continuous input current of the power converter (*CCM*). Besides that, it can be seen that the current in inductor L_2 presents a similar behaviour of the one in inductor L_1, ensuring also *CCM*. Regarding the output currents, i_{o1} and i_{o2} in Fig. 8, it is shown they are well balanced as they have the same average and ripple values. Therefore, the proposed converter will contribute to balance the voltages of bipolar *DC* microgrids.

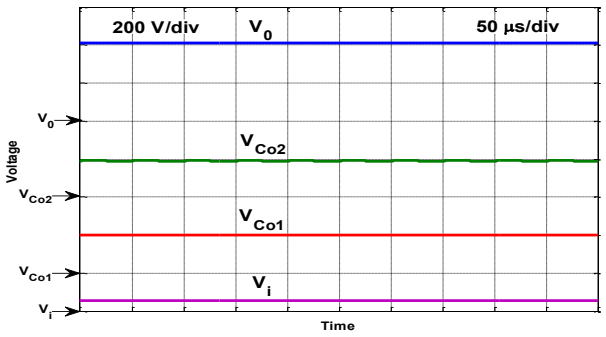

FIGURE 6. Simulation waveforms of the input (V_i) and output (V_o, V_{Co1} and V_{Co2}) voltages of the power converter.

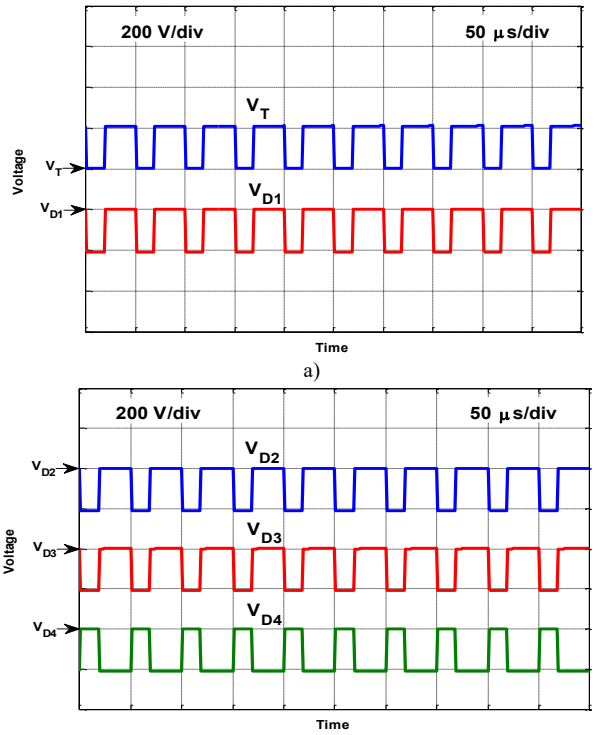

FIGURE 7. Simulation waveforms of the voltages across the power devices.

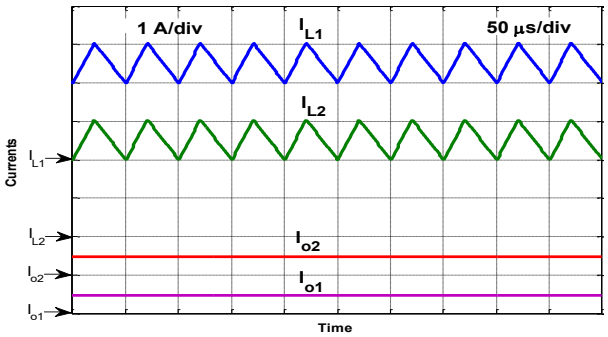

FIGURE 8. Simulation waveforms of the input current (i_{L1}), inductor current (i_{L2}); output currents i_{o1} and i_{o2}.

To test the capability of the proposed converter to inject the power in an asymmetric way into the two poles in an unbalanced situation, a new simulation with an unbalanced resistive load was also realized. For this simulation, it was initially considered the circuit with a balanced load (540 Ω and 540 Ω). However, suddenly the resistor connected to the negative pole changed to 190 Ω originating in this way an asymmetry in the circuit output. The obtained output voltages in this test can be seen in Fig. 9. This result shows that although the load became unbalanced, the output pole voltages remain balanced. Despite using only one switch, the output currents appear in this situation as unbalanced (Fig. 10). Moreover, the output current connected to the pole with a higher load (i_{o2}) has higher value contributing in this way to balance the microgrid voltages.

This article has been accepted for publication in a future issue of this journal, but has not been fully edited. Content may change prior to final publication. Citation information: DOI 10.1109/ACCESS.2021.3122877, IEEE Access

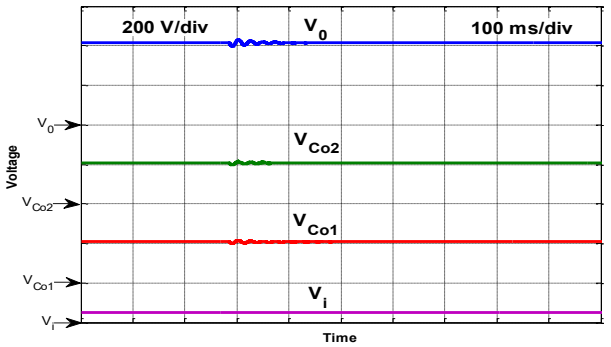

FIGURE 9. Simulation waveforms of the input (V_i) and output (V_o, V_{Co1} and V_{Co2}) voltages, for a suddenly change in the load of the negative pole.

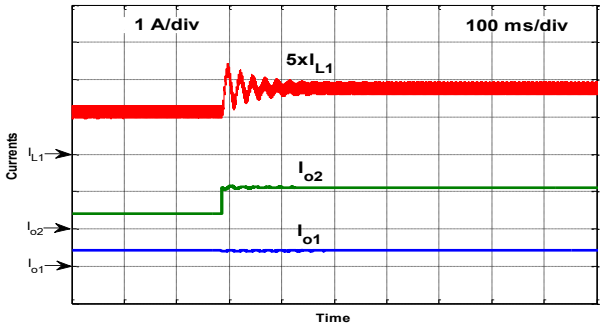

FIGURE 10. Simulation waveforms of the output currents (i_{o1} and i_{o2}), for the situation of a suddenly change in the load of the negative pole.

B. EXPERIMENTAL TESTS

The results obtained from the experimental tests realized through the developed prototype are presented in Figs. 11 to 13. As shown by Fig. 11 the output voltage was set for 400 V. This voltage was obtained for a duty cycle of 0.36. From this is possible to see that output/input voltage gain is near to the expected theoretical gain. This figure also shows the output capacitors voltages (V_{o1} and V_{o2}) of the power converter, being possible to confirm that they are practically half of the total output voltage. The confirmation about the reduction of the voltages across the power devices when compared with the output voltage of the converter can be seen in Fig. 12. From these voltages waveforms it is possible to see that the maximum voltage that they must hold-off is half of the total output voltage, confirming in this way the theoretical expectations.

The confirmation about the main currents in the circuit can be seen in Fig. 13. From the analysis of the waveforms of the experimental currents it is possible to see that the input current (also in the inductor L_1) presents a continuous conduction mode. The waveform of the experimental current in inductor L_2 also shows a similar behaviour with the one in inductor L_1. This figure also shows that the output currents (i_{o1} and i_{o2}) are balanced, like in the simulation. This confirms that in a situation of a balanced DC microgrid the proposed converter will not contribute to its unbalance.

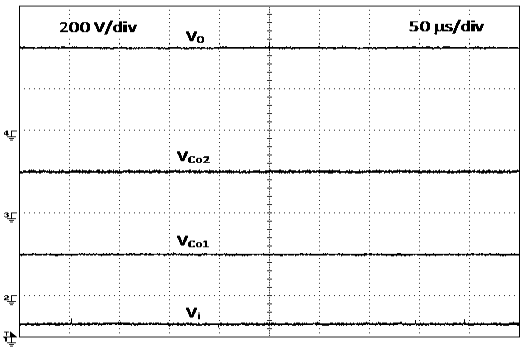

FIGURE 11. Experimental waveforms of the input (V_i) and outputs (V_o, V_{Co1} and V_{Co2}) voltages of the power converter.

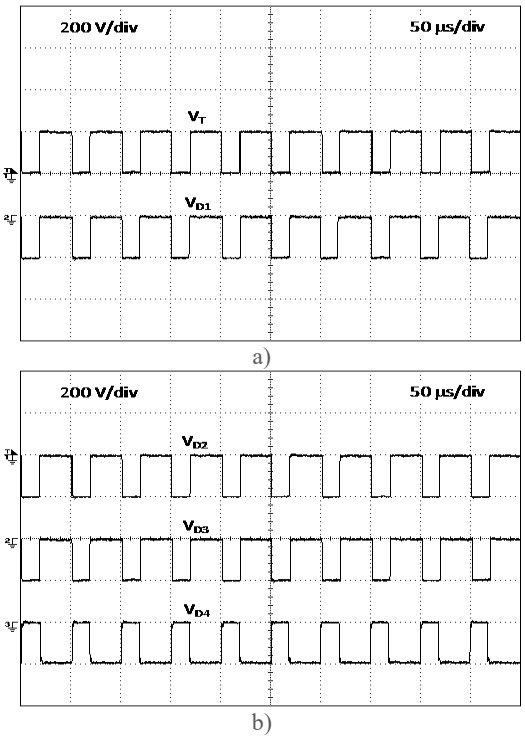

FIGURE 12. Experimental waveforms of the voltages across the power semiconductors.

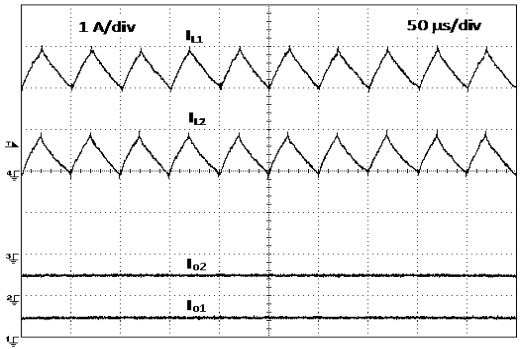

FIGURE 13. Experimental waveforms of the input current (i_{L1}) and inductor current (i_{L2}).

This article has been accepted for publication in a future issue of this journal, but has not been fully edited. Content may change prior to final publication. Citation information: DOI 10.1109/ACCESS.2021.3122877, IEEE Access

To experimentally confirm the capability of the proposed converter to help in balancing the bipolar microgrid, a test with an unbalanced resistive load was also performed. For this test, an initially balanced load (with a resistor of 540 Ω in each of the poles) was suddenly unbalanced by paralleling an extra load in the negative pole (to 190 Ω). Fig. 14 shows the input and output voltages of the converter. The waveforms of the positive and negative poles (V_{Co1} and V_{Co2}) show that they maintain the same voltage value even when the load is unbalanced. This is ensured by the asymmetrical injection of the converter output currents (i_{o1} and i_{o2}) as shown in Fig. 15. Indeed, the experimental waveforms of the converter output currents shows that when the load became unbalanced the currents also became unbalanced, since the output connected to the pole with higher load presents a higher value. This confirms that in an unbalanced situation the converter will inject in an asymmetric way the power into the two poles of the microgrid helping their balance, using only a single switch.

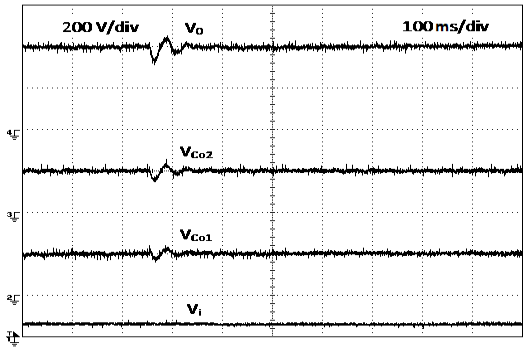

FIGURE 14. Experimental waveforms of the input (V_i) and output (V_o, V_{Co1} and V_{Co2}) voltages, for the situation of a suddenly change in the load of the negative pole.

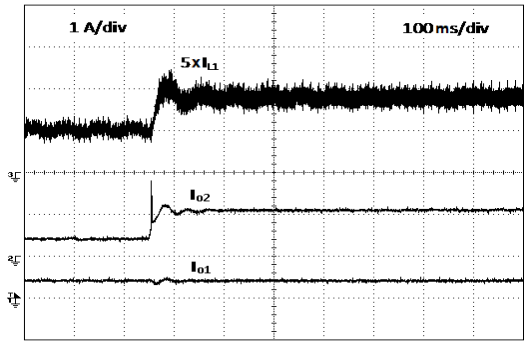

FIGURE 15. Experimental waveforms of the output currents (i_{o1} and i_{o2}), for the situation of a suddenly change in the load of the negative pole.

VII. CONCLUSION

This study proposed a novel *DC-DC* power converter topology that is especially suited for bipolar *DC* microgrids or transformerless grid-connect *PV* and fuel cell generators. The suitability to these applications is due to the fact that the topology is characterized by a double output, allowing connections to the positive, neutral and negative poles of bipolar microgrids. The proposed converter contributes to balance the voltages of the microgrid. The topology is also characterized by a high input-output voltage gain and continuous input current, which is very important for *RES* such as *PV* and fuel cell generators. The proposed *DC-DC* converter was developed with the purpose to maintain, as must as possible a reduced number of components, using only a single active switch. One of the features of the proposed *DC-DC* is the ability to create an output midpoint that is directly connected to the ground of the input *DC* power supply avoiding the common mode leakage current. The operating principles of the proposed *DC-DC* converter, as well, their component sizing were also presented. The assumptions, theoretical analysis and design were verified through the experimental results obtained from a laboratory setup.

REFERENCES

[1] N. Bizon, N. M. Tabatabaei, F. Blaabjerg and E. Kurt. “Energy Harvesting and Energy Efficiency: Technology, Methods, and Applications”. Lecture notes in Energy. Springer AG. ISBN: 978-3-319-49874-4, 2017.

[2] Y. Yang, K. A. Kim, F. Blaabjerg, and A. Sangwongwanich. “Advances in Grid-Connected Photovoltaic Power Conversion Systems”. Springer. ISBN: 978-0-08-102339-6.

[3] M. S. Agamy et al., "A High-Power-Density DC–DC Converter for Distributed PV Architectures," in IEEE Journal of Photovoltaics, vol. 3, no. 2, pp. 791-798, April 2013.

[4] H-S. Lee, J-J. Yun, “High-Efficiency Bidirectional Buck–Boost Converter for Photovoltaic and Energy Storage Systems in a Smart Grid”, IEEE Trans. Power Electr., vol 34, no. 5, pp. 4316-4328, May 2019.

[5] S. Inoue, H. Akagi, “A bidirectional dc-dc converter for an energy storage system with galvanic isolation,” IEEE Trans. Power Electron., vol. 22 (6), pp.2299-2306, Nov. 2007.

[6] M. W. Beraki, J. P. F. Trovão, M.S. Perdigão, and M. R. Dubois, “Variable Inductor Based Bidirectional DC–DC Converter for Electric Vehicle,” IEEE Trans. Veh. Technol., vol. 66, no. 10, pp. 8764-8772, Oct. 2017.

[7] L. Tan, B. Wu, S. Rivera and V. Yaramasu, “Comprehensive DC Power Balance Management in High-Power Three-Level DC–DC Converter for Electric Vehicle Fast Charging,” IEEE Trans. Power Electr., vol. 31, no. 1, pp. 89-100, Jan. 2016.

[8] M. Z. Hossain, N.A. Rahim and J. Selvaraj, Recent progress and development on power DC DC converter topology, control, design and applications: a review, Elsevier, Renewable and Sustainable Energy Reviews, vol. 81, pp. 205-230, Jan. 2018.

[9] J.-M. Shen, H.-L. Jou, J.-C. Wu, "Novel transformerless gridconnected power converter with negative grounding for photovoltaic generation system", IEEE Trans. Power Electron., vol. 27, no. 4, pp. 1818-1829, Apr. 2012.

[10] M. Forouzesh, Y. P. Siwakoti, S. A. Gorji, F. Blaabjerg, B. Lehman, “Step-Up DC-DC Converters: A Comprehensive Review of Voltage-Boosting Techniques, Topologies, and Applications”, IEEE Trans. Power Electron, vol. 32, no.12, pp. 9143-9178, Dec. 2017.

[11] A. Emrani, E. Adib, and H. Farzanehfard, “Single-switch soft switched isolated dc-dc converter”, IEEE Trans. Power Electron. vol. 27, no. 4, pp. 1952-1957, Apr.2012.

[12] H. Tarzamni, F. Tahami, M. Fotuhi-Firuzabad and F. Blaabjerg, "Improved Markov Model for Reliability Assessment of Isolated Multiple-Switch PWM DC-DC Converters," in IEEE Access, vol. 9, pp. 33666-33674, 2021.

[13] O. Husev, L. Liivik, F. Blaabjerg, A. Chub, D. Vinnikov, I. Roasto, “Galvanically Isolated Quasi-Z-Source DC-DC Converter with a

Novel ZVS and ZCS Technique", IEEE Trans. Ind. Electron., vol. 62, no. 12, pp. 7547-7555, Dec. 2015.
[14] H. Wang, Q. Sun, H. S. H. Chung, S. Tapuchi, A. Ioinovici, "A ZCS Current-Fed Full-Bridge PWM Converter with Self-Adaptable Soft-Switching Snubber Energy", IEEE Trans. Power Electron., vol. 24, no. 8, pp. 1977-1991, Aug. 2009.
[15] Y. Jang and M. Jovanovic, "Isolated boost converter", IEEE Trans. Power Electron., vol. 22, no. 4, pp. 1514 1521, Jul. 2007 .
[16] M-K. Nguyen, T-D. Duong, Y-C. Lim and Y-J. Kim, "Isolated Boost DC-DC Converter with Three Switches", IEEE Trans. Ind. Electron., vol. 33, no. 2, pp. 1389-1398, Feb.2018.
[17] S.A. Gorji, M. Ektesabi, J. Zheng, "Isolated switched-boost push-pull DC–DC converter for step-up applications," IET Electronics Letters, vol. 53, no.3, pp. 117-119. Feb. 2017.
[18] H. Jahangiri, S. Mohammadpour, A. Ajami, "A high step-up DC-DC boost converter with coupled inductor based on quadratic converters," in Proc. 9th Annual Power Electronics, Drives Systems and Technologies Conference, pp. 13-15, Feb. 2018.
[19] M. Sagar Bhaskar et al., "Survey of DC-DC Non-Isolated Topologies for Unidirectional Power Flow in Fuel Cell Vehicles," in IEEE Access, vol. 8, pp. 178130-178166, 2020.
[20] V. F. Pires, D. Foito, F. R. B. Batista, J. F. Silva, "A photovoltaic system with a DC/DC converter based on an integrated Boost-Cuk generator topology", Elsevier, Solar Energy, vol. 136, pp. 1-9, Oct. 2016.
[21] S.-W. Lee, H.-L. Do, "Zero-Ripple Input-Current High-Step-Up Boost–SEPIC DC–DC Converter With Reduced Switch-Voltage Stress", IEEE Trans. on Power Electronics, vol. 32, no. 8, pp. 6170-6177, Aug 2017.
[22] R. Moradpour, H. Ardi, A. Tavakoli, "Design and Implementation of a New SEPIC-Based High Step-Up DC/DC Converter for Renewable Energy Applications", IEEE Trans. on Ind. Elect., vol. 65, no. 2, pp. 1290-1297, Feb. 2018.
[23] A. Abramovitz and K. M. Smedley, "Analysis and design of a tapped inductor buck-boost PFC rectifier with low bus voltage", IEEE Trans. Power Electron., vol. 26, no. 9, pp. 2637-2649, Sept.2011.
[24] H. Liu, H. Hu, H. Wu, Y. Xing, I. Batarseh, "Overview of High-Step-Up Coupled-Inductor Boost Converters", IEEE Journal of Emerging and Selected Topics in Power Electronics, vol. 4, no. 2, pp. 689-704, Feb. 2016.
[25] Y. Ye and K. W. E. Cheng, "A family of single-stage switched-capacitor- inductor PWM converters", IEEE Trans. Power Electron., vol. 28, no. 11, pp. 5196-5205, Feb. 2013.
[26] P. K. Peter and V. Agarwal, "Current Equalization in Photovoltaic Strings With Module Integrated Ground-Isolated Switched Capacitor DC–DC Converters," in IEEE Journal of Photovoltaics, vol. 4, no. 2, pp. 669-678, March 2014.
[27] X. Wu, W. Shi and J. Du, "Dual-Switch Boost DC–DC Converter for Use in Fuel-Cell-Powered Vehicles," in IEEE Access, vol. 7, pp. 74081-74088, 2019.
[28] D. Bao, A. Kumar, X. Pan, X. Xiong, A. R. Beig and S. K. Singh, "Switched Inductor Double Switch High Gain DC-DC Converter for Renewable Applications," in IEEE Access, vol. 9, pp. 14259-14270, 2021.
[29] D. R. Espinoza Trejo, S. Taheri, J. L. Saavedra, P. Vázquez, C. H. De Angelo and J. A. Pecina-Sánchez, "Nonlinear Control and Internal Stability Analysis of Series-Connected Boost DC/DC Converters in PV Systems With Distributed MPPT," in IEEE Journal of Photovoltaics, doi: 10.1109/JPHOTOV.2020.3041237.
[30] M. Zhu and F. L. Luo, "Series SEPIC implementing voltage-lift technique for DC-DC power conversion", IET Power Electron., vol. 1, no. 1, pp. 109-121, Mar. 2008.
[31] M. S. Bhaskar, D. J. Almakhles, S. Padmanaban, F. Blaabjerg, U. Subramaniam and D. M. Ionel, "Analysis and Investigation of Hybrid DC–DC Non-Isolated and Non-Inverting Nx Interleaved Multilevel Boost Converter (Nx-IMBC) for High Voltage Step-Up Applications: Hardware Implementation," in IEEE Access, vol. 8, pp. 87309-87328, 2020.
[32] A. M. S. S. Andrade, M. L. da S. Martins, "Quadratic-Boost with Stacked Zeta Converter for High Voltage Gain Applications", IEEE Journal of Emerging and Selected Topics in Power Electronics, vol. 5, no. 4, pp. 1787-1796, Jun. 2017.
[33] V. F. Pires, D. Foito, A. Cordeiro, "A DC-DC Converter with Quadratic Gain and Bidirectional Capability for Batteries/Supercapacitors", IEEE Trans. Ind. Appl., vol. 54, no. 1, pp. 274-285, Sept. 2018.
[34] J. C. Rosas-Caro, V. M. Sanchez, J. E. Valdez-Resendiz, J. C. Mayo-Maldonado, F. Beltran-Carbajal, A. Valderrabano-Gonzalez, "Quadratic boost converter based on stackable switching stages", IET Power Electron., vol. 11, no. 8, pp. 1373-1381, Jun. 2018.
[35] J. Liu, J. Wu, J. Qiu and J. Zeng, "Switched Z-Source/Quasi-Z-Source DC-DC Converters With Reduced Passive Components for Photovoltaic Systems," in IEEE Access, vol. 7, pp. 40893-40903, 2019.
[36] J. Zhao, D. Chen and J. Jiang, "Transformerless High Step-Up DC-DC Converter With Low Voltage Stress for Fuel Cells," in IEEE Access, vol. 9, pp. 10228-10238, 2021.
[37] W. Li and X. He, "Review of nonisolated high-step-up DC/DC converters in photovoltaic grid-connected applications", IEEE Trans. Ind. Electron., vol. 58, no. 4, pp. 1239-1250, May. 2011.
[38] H. Kakigano, Y. Miura, T. Ise, "Low-Voltage Bipolar-Type DC Microgrid for Super High Quality Distribution," IEEE Trans. Power Electron., vol. 25, no. 12, pp. 3066-3075, Dec. 2010.
[39] F. Wang, Z. Lei, X. Xu, X. Shu, "Topology Deduction and Analysis of Voltage Balancers for DC Microgrid", IEEE Journal Emerg. and Selected Topics in Power Electr., vol. 5, no. 2, pp. 672-680, Jun. 2017.
[40] J. Lee, Y. Cho, J. Jung, "Single-Stage Voltage Balancer with High-Frequency Isolation for Bipolar LVDC Distribution System", IEEE Trans. Ind. Electron., vol 65, no. 5, pp. 3596 - 3606, May 2020.
[41] M. B. Ferrera, S. P. Litrán, E. D. Aranda, J. M. Márquez, "A Converter for Bipolar DC Link Based on SEPIC-Cuk Combination", IEEE Trans. Power Electron., vol 30, no. 12, pp. 6483-6487, Dec. 2015.
[42] Y. Zhang, L. Zhou, M. Sumner, P. Wang, "Single-Switch, Wide Voltage-Gain Range, Boost DC–DC Converter for Fuel Cell Vehicles", IEEE Trans. on Vehicular Technology, vol. 67, no. 1, pp. 134-145, Jan 2018.
[43] V. F. Pires, D. Foito, J. F. Silva, "A single switch hybrid DC/DC converter with extended static gain for photovoltaic applications", Electric Power Systems Research, vol. 146, pp. 228-235, May2017.
[44] A. K. Mishra, B. Singh, "Solar Photovoltaic Array Dependent Dual Output Converter Based Water Pumping Using Switched Reluctance Motor Drive", IEEE Trans. Industry Applications, vol. 53, no. 6, pp. 5615-5623, Nov./Dec. 2017.
[45] K. Nathan, S. Ghosh, Y. Siwakoti, T. Long, "A New DC–DC Converter for Photovoltaic Systems: Coupled-Inductors Combined Cuk-SEPIC Converter", IEEE Trans. Energy Conversion, vol 34, no. 1, pp. 191-201, Mar. 2019.
[46] S. Rezayi, H. Iman-Eini, M. Hamzeh, S. Bacha, S. Farzamkia, "Dual-output DC/DC boost converter for bipolar DC microgrids", IET Renewable Power Generation, vol. 13, no. 8, pp. 1402-1410, June 2019.